

PDF hosted at the Radboud Repository of the Radboud University Nijmegen

The following full text is a publisher's version.

For additional information about this publication click this link.

<http://hdl.handle.net/2066/48680>

Please be advised that this information was generated on 2019-02-17 and may be subject to change.

Localization and Functional Characterization of Glycosaminoglycan Domains in the Normal Human Kidney as Revealed by Phage Display–Derived Single Chain Antibodies

Joost F.M. Lensen,* Angelique L.W.M.M. Rops,[†] Tessa J.M. Wijnhoven,*[‡] Theo Hafmans,*[§] Wouter F.J. Feitz,^{||} Egbert Oosterwijk,^{||} Bernhard Banas,[¶] René J.M. Bindels,** Lambert P.W.J. van den Heuvel,[‡] Johan van der Vlag,[†] Jo H.M. Berden,[†] and Toin H. van Kuppevelt*

Departments of *Biochemistry, [†]Nephrology, [‡]Pediatrics, [§]Pulmonary Diseases, ^{||}Pediatric Urology, and **Physiology, Radboud University Nijmegen Medical Center, NCMLS, Nijmegen, The Netherlands; and [¶]Department of Internal Medicine II, Nephrology, University of Regensburg, Regensburg, Germany

Glycosaminoglycans (GAG) play an important role in renal homeostasis. They are strongly negatively charged polysaccharides that bind and modulate a myriad of proteins, including growth factors, cytokines, and enzymes. With the aid of specific phage display–derived antibodies, the distribution of heparan sulfate (HS) and chondroitin sulfate (CS) domains in the normal human kidney was studied. HS domains were specifically located in basement membranes and/or surfaces of renal cells and displayed a characteristic distribution over the nephron. A characteristic location in specific parts of the tubular system was also observed. CS showed mainly an interstitial location. Immunoelectron microscopy indicated specific ultrastructural location of domains. Only partial overlap with any of seven different proteoglycan core proteins was observed. Two HS domains, one highly sulfated (defined by antibody HS4C3) and one low sulfated (defined by antibody RB4Ea12), were studied for their cell biologic relevance with respect to the proliferative effect of FGF-2 on human mesangial cells *in vitro*. Fibroblast growth factor 2 (FGF-2) binding was HS dependent. Addition of purified HS4C3 antibody but not of the RB4Ea12 antibody counteracted the binding and the proliferative effect of FGF-2, indicating that the HS4C3 domain is involved in FGF-2 handling by mesangial cells. In conclusion, specific GAG domains are differentially distributed in the normal human kidney and are likely involved in binding of effector molecules such as FGF-2. The availability of tools to identify and study relevant GAG structures allows the development of glycomimetics to halt, for instance, mesangial proliferation and matrix production as seen in diabetic nephropathy.

J Am Soc Nephrol 16: 1279–1288, 2005. doi: 10.1681/ASN.2004050413

Glycosaminoglycans (GAG) are polysaccharides that are produced in virtually every cell of the human body and are secreted into the extracellular matrix or retained at the cell surface. The GAG precursor polysaccharide undergoes a series of modification reactions, resulting in very complex structures. GAG chains are generally attached to core proteins, forming proteoglycans (1). Major GAG classes include heparan sulfates/heparin (HS/hep), dermatan sulfates (DS), and chondroitin sulfates (CS). GAG are involved in a myriad of processes, such as growth factor binding, signal transduction, and cell adhesion (2–4).

The importance of GAG in the kidney has been demon-

strated, among others, by knockout studies. Mice deficient for the enzyme that catalyzes the 2-O-sulfation of HS (2-O-sulfotransferase) demonstrate agenesis of kidneys (5). The same holds for mice that lack the enzyme glucuronyl C5-epimerase, which catalyzes the change of glucuronic acid to iduronic acid (IdoA) residues (6).

A mutation in the gene encoding glypican-3 (a membrane-bound heparan sulfate proteoglycan) manifests itself by cystic and dysplastic kidneys in men (Simpson-Golabi-Behmel syndrome), as well as in mice (7). Alterations in GAG composition and/or content have been observed in a large number of renal pathologies, including diabetic nephropathy, glomerulonephritides, nephroblastoma (Wilms' tumor), amyloidosis, polycystic kidney disease, minimal-change nephropathy, and Denys-Drash syndrome (8–13). The involvement of GAG, especially HS, in such a diverse group of pathologies suggests the presence of a large number of structurally different GAG in the kidney.

The biosynthesis of GAG allows for a large number of dif-

Received May 26, 2004. Accepted February 4, 2005.

Published online ahead of print. Publication date available at www.jasn.org.

Address correspondence to: Dr. Toin H. van Kuppevelt, Department of Biochemistry 194, NCMLS, Radboud University Nijmegen Medical Center, P.O. Box 9101, 6500 HB Nijmegen, The Netherlands. Phone: +31-24-3616759; Fax: +31-24-3540339; E-mail: a.vankuppevelt@ncmls.ru.nl

ferent GAG chains as well as for extensive structural heterogeneity within one chain. For example, HS consists of repeating disaccharide units that contain a uronic acid (UA), which can be either D-glucuronic acid (GlcA) or IdoA, with or without 2-O-sulfation, and a glucosamine residue, which can be N-acetylated (NAc), N-sulfated (NS), or N-unsubstituted. In addition, the glucosamine residue can be 3- and/or 6-O-sulfated. A number of different HS disaccharides have been found in the kidney, including GlcA-GlcNR (R can be an acetyl or a sulfate group), IdoA-GlcNR, GlcA2S-GlcNR, IdoA2S-GlcNR, GlcA-GlcNR6S, IdoA-GlcNR6S, and IdoA2S-GlcNR6S (14–16). Furthermore, N-unsubstituted glucosamine (GlcNH₂) residues are found in the kidney and account for approximately 2% of the total disaccharide units present (17). With combinations of these disaccharides and with the knowledge that an HS chain consists of 40 to 160 disaccharides, there can be a vast number of different HS chains, each with unique disaccharide sequences.

Studies of alterations in GAG associated with renal pathology have generally been limited to the analysis of total GAG content or their major classes. Studies of the topology and domain structure of GAG have been hampered by a lack of appropriate tools that allow detection of the different GAG domains. Only a few antibodies against these GAG domains are available, for instance the JM403 antibody (18). We recently obtained specific tools to analyze GAG heterogeneity by selecting a large number of phage display–derived antibodies that are reactive with renal GAG (19–21).

In this study, we used a panel of these specific antibodies selected against HS and one against CS to establish the topography of GAG domains in human kidney. Furthermore, the significance of two HS domains in growth factor handling by human mesangial cells (HMC) *in vitro* was studied.

Materials and Methods

Antibodies

Phage Display–Derived Anti-HS Antibodies. The antibodies used in this study (further referred to as scFv antibodies) were obtained

using the phage-display technique, and some of their characteristics are shown in Table 1.

Antibodies Specific for Renal Tubules. For studying the distribution of GAG domains and core proteins over the nephron, the following renal tubule–specific antibodies (see Table 2) were applied: Aquaporin 1, 2, and 3; RCK-105 (keratin 7); Tamm Horsfall; and Calbindin D_{28k}.

Human Kidney Specimens

Adult human kidneys ($n = 9$; one female, eight male; average age, 50.7 ± 5.0 yr; range, 40 to 56 yr) were obtained after surgical removal for renal cell carcinoma. Whole kidneys were excised, and normal tissue was selected after macro- and microscopic evaluation. Patients did not have any other kidney disease.

Immunohistochemical Localization of GAG Domains

Cryosections (5 μ m) were cut, air dried, blocked for 10 min with PBS that contained 2% (wt/vol) BSA, and incubated with primary antibody for 90 min at 22°C. ScFv antibodies were detected by incubation with rabbit anti-VSV antibodies (MBL, Nagoya, Japan) or mouse anti-VSV antibodies (P5D4, culture supernatant), followed by Alexa 488– or Alexa 594–conjugated goat anti-rabbit or goat anti-mouse IgG (Molecular Probes, Leiden, The Netherlands; 1:100 in PBS that contained 2% BSA), all for 60 min at 22°C. Antibodies against distinct segments of the renal tubular system were visualized using Alexa 488– or Alexa 594–conjugated goat anti-mouse or goat anti-rabbit IgG antibodies (1:100 in PBS that contained 2% BSA), for 60 min at 22°C. After each incubation, sections were washed in PBS (three times for 5 min). As a control, the irrelevant scFv antibody MPB59 was used. This scFv antibody does not stain human kidney tissue. Additional controls were the omission of primary, secondary, or conjugated antibody. After the last washing step, cryosections were fixed in 100% ethanol for 20 s, air-dried, and embedded in Mowiol.

Immunohistochemical Localization of Core Proteins

For the immunohistochemical localization of core proteins, the same protocol as for the localization of GAG domains was used but with omission of the anti-VSV antibodies. Antibodies used were anti-versican (12C5; Development Studies Hybridoma bank; 1:50), anti-perlecan (Chemicon, Temecula, CA; 1:10,000), anti-agrin (UBI, Lake Placid, NY;

Table 1. Characteristics of the different GAG domain–specific scFv antibodies^a

scFv Antibody ^b	V _H Family	DP Gene Segment	V _H CDR3 Sequence	Class of GAG Recognized	Reference	Preferred Chemical Group
HS4C3	3	38	GRRLKD	HS	19	IdoA2S-GlcNS3S6S
HS4E4	3	38	HAPLRNTRTNT	HS	21	N-sulfation, probably no 6–0 sulfation
AO4B08	3	47	SLRMNGWRAHQ	HS	21	IdoA2S-GlcNS6S
RB4Ea12	3	32	RRYALDY	HS	21	IdoA-GlcNS6S
EW4A11	3	38	ERNTIRR	HS	20	N-sulfation + O-sulfation
EW3D10	3	38	GRTVGRN	HS	20	Primarily O-sulfation
IO3H10	1	7	AKRLDW	CS	45	GlcA-GalNAc6S
MPB59	3	38	HRRLSP	— (control)	—	—

^aGiven are the scFv antibody code, DP gene number, V_H germ line gene family, amino acid sequence of the V_H complementarity determining region 3 (CDR3), the class of GAG with which the antibody reacts, and the preferred chemical group. GAG, glycosaminoglycans; HS, heparan sulfate; CS, chondroitin sulfate.

^bAll scFv antibodies recognize different epitopes as based on different staining patterns and different reactivity toward various HS/CS preparations (19–21;45) (unpublished data).

Table 2. Overview of antibodies specific for renal tubules used in this study^a

Antibody	Segment Recognized	Origin	Dilution	Reference
Anti-aquaporin 1	PT and DTL	Mouse	1:250	46, 47
Anti-aquaporin 2	CD	Rabbit	1:100	46, 47
Anti-aquaporin 3	CD (basolateral membrane)	Rabbit	1:100	46, 47
Anti-rck-105	Loop of Henle	Mouse	1:50	48
Anti-Tamm-Horsfall	TAL	Goat	1:600	49
Anti-calbindin D _{28k}	CNT	Mouse	1:100	50

^aPT, proximal tubule; DTL, descending thin limb; CD, collecting duct; TAL, thick ascending limb; CNT, connecting tubule.

1:20), anti-endostatin (the c-terminal part of type XVIII collagen; Alpha Diagnostic International, San Antonio, TX; 1:100), anti-syndecan-1 (CD138; Serotec Inc., Oxford, UK; 1:100), -2 (10H4, 1:500) and -3 (1C7, 1:50). Antibodies were visualized using Alexa 488- or Alexa 594-conjugated secondary antibodies.

A confocal microscope (Biorad MRC1024) and a routine immunofluorescence microscope (Zeiss Axioskop) were used to analyze the sections. Two observers (J.F.M.L. and A.R.) analyzed the stainings double blind.

Immunoelectron Microscopy

Human kidney biopsies were fixed for 3 h in Somogyi solution that contained 4% formaldehyde and 0.05% glutaraldehyde in 0.1 M phosphate buffer. Sections (200 μ m) were cut using a vibratome and incubated in increasing amounts of glycerol (10 to 30%) in phosphate buffer for 30 min. Sections were oriented on Thermanox (LAB-TEK DVI; Miles Laboratories Inc., Naperville, IL) and rapidly frozen in liquid propane (-190°C), using a rapid freeze apparatus (KF80; Reichert-Jung, Wetzlar, Germany). Freeze substitution was performed as described (22). Ultrathin lowicryl HM20 resin sections were cut on a Reichert Ultracut-E and mounted on one-hole nickel grids coated with a formvar film. Sections were preincubated in PBS that contained 0.2% BSA and 0.05% cold fish skin gelatin (PBG). Sections were incubated overnight at 4°C in drops of PBG that contained anti-GAG scFv antibodies, diluted 1:100, and washed for 20 min in PBG. Bound antibodies were visualized using anti-VSV tag antibody P5D4 and goat anti-mouse IgG labeled with gold spheres (10 nm; Aurion, Wageningen, Netherlands). Sections were washed in PBS and postfixed with 2.5% glutaraldehyde in PBS for 5 min. After washing with distilled water, sections were contrasted with uranyl acetate and studied using a Jeol TEM 1010 electron microscope.

Involvement of HS Domains in Fibroblast Growth Factor 2 Handling

Binding of Fibroblast Growth Factor 2 to HS. For studying whether fibroblast growth factor 2 (FGF-2; produced, isolated, and purified as described before [23]) binds to HS, two strategies were used. In the first strategy, cryosections were incubated with and without FGF-2 (10 μ g/ml PBS that contained 1% Tween) for 1 h and subsequently stained for HS domains using scFv antibodies (see above). We evaluated whether staining intensity was reduced. In addition, before incubation with FGF-2, cryosections were incubated for 2 h with 0.04 IU of heparinase III (IBEX Technologies, Montreal, QU, Canada) in 25 mM Tris/HCl (pH 8) at 22°C. Thereafter, the capacity to bind FGF-2 was evaluated by immunofluorescence using an anti-FGF-2 antibody (F-3393; Sigma-Aldrich, St. Louis, MO) and Alexa 488-conjugated goat anti-mouse IgG.

In the second approach, the effect of purified scFv antibodies on

FGF-2 binding to human mesangial cells in culture was studied. SV40 large T antigen-immortalized HMC were used as described before (24) and grown in DMEM (Invitrogen, Breda, The Netherlands) with 5.5 mM glucose and 10% heat-inactivated FCS gold (PAA, Pasching, Austria) at 37°C, unless stated otherwise. Passages 5 to 8 were used for the experiments. Cells were evaluated for the expression of mesangial cell markers, positive ones (smooth muscle actin, fibronectin, vimentin, and desmin) as well as negative ones (cytokeratin 18, and CD45). Results were the same as found by Banas *et al.* (24). In 24-well plates (Greiner, Alphen a/d Rijn, The Netherlands), HMC were seeded on glass coverslips at a density of 50,000 cells/well. After 24 h of adjusting, the cells were washed twice with PBS and once with DMEM that contained 0.5% FCS. Cells then were incubated for 5 min, 30 min, 60 min, and 24 h in DMEM that contained 100 μ g of purified scFv antibodies/ml DMEM that contained 0.5% FCS, followed by incubation for 1 h in DMEM that contained FGF-2 (10 ng/ml). Cells were fixed using ice-cold methanol and stained with scFv antibodies as described or with the anti-FGF-2 antibody followed by goat anti-mouse Alexa 488. For evaluating HS dependence of scFv antibody binding as well as FGF-2 binding, cells were pretreated with heparinase III (see above).

Involvement of HS Domains in FGF-2-Induced Cell Proliferation.

For evaluating the effect of the scFv antibodies on the FGF-2-induced proliferation, HMC were seeded in a 96-well plate (Greiner; 10,000 cells/well) in DMEM that contained 5.5 mM glucose and 0.5% FCS. Cells were incubated at 37°C with and without purified scFv antibodies as described above, and FGF-2 (10 ng/ml) was added 5 min thereafter. Incubation was for 4 d. Cell proliferation was analyzed using the WST-1 test, based on the conversion of the substrate WST-1 by mitochondrial dehydrogenases of viable cells to a soluble formazan salt, which directly correlates with the cell number (Roche Diagnostics GmbH, Penzberg, Germany). Absorbance was read at 450 nm.

Results

Localization of GAG Domains

Immunofluorescence Microscopy. The distribution of GAG domains in human kidney is summarized in Table 3. Heparinase III treatment abolished all HS staining (data not shown). HS domains were restricted to basement membranes or cell surfaces, whereas the CS domain primarily localized to the interstitium (Figures 1 and 2, Table 3). Of the anti-HS scFv antibodies, HS4C3 predominantly stained the mesangial areas and peritubular capillaries but also showed staining of the glomerular basement membrane (GBM; Figures 1 through 3, Table 3). The domain recognized by HS4E4 was primarily present in Bowman's capsule and the collecting ducts (Figure 1, Table 3). ScFv antibody AO4B08 most strongly stained the collecting ducts and smooth muscle cells, but there was also

Table 3. Distribution of GAG domains in the normal human kidney as detected by scFv antibodies against HS or CS^a

Morphologic Structure	HS						CS
	scFv antibody	HS4C3	HS4E4	AO4B08	RB4Ea12	EW4A11	EW3D10
Glomerular capillary wall	+	–	–	–	±	+	–
Bowman's capsule	–	++	+	–	±	–	+
Mesangium	++	–	–	–	±	+	–
PT	±	+	–	+	+ ^b	–	+
DTL	±	–	+	–	+	–	–
Ascending thin limb	±	–	+	–	+	–	–
TAL	±	–	–	–	±	–	+
CNT	±	±	+	+	+	+	±
CD	+	++	++	+	+	++	±
Peritubular capillaries	++	–	–	–	±	+	–
Smooth muscle cells	–	+	++	–	±	–	±
Blood vessel endothelium	±	–	–	+	±	–	+

^aStaining: ++, strong; +, good; ±, moderate; and –, absent.

^bParts of the tubule stained positive.

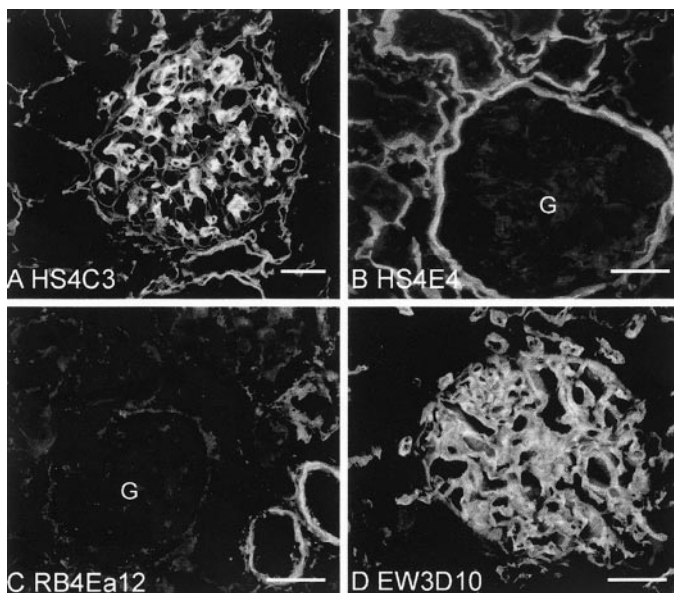


Figure 1. Immunostaining for heparan sulfate (HS) domains in the normal human glomerulus using four different anti-glycosaminoglycans (anti-GAG) scFv antibodies. Cryosections were incubated with periplasmic fractions of bacteria that contained the antibodies. The antibodies shown are HS4C3 (A), HS4E4 (B), RB4Ea12 (C), and EW3D10 (D). G, glomerulus. Bar = 50 μ m.

good staining of the descending and ascending thin limbs of Henle's loop (Figure 2, Table 3) and Bowman's capsule. RB4Ea12 showed good staining only of the proximal tubules (Figure 1, Table 3). EW4A11 moderately stained all structures within the glomerulus and the thick ascending limb but also showed clear staining of the rest of the tubules (Table 3). EW3D10 displayed a strong staining of the collecting ducts and an evident staining of the glomerular tuft, the mesangium, peritubular capillaries, and the connecting tubules (Figures 1 and 2, Table 3).

IO3H10, the anti-CS scFv antibody, stained the proximal tubules and the thick ascending limbs, as well as Bowman's capsule and blood vessel endothelium (Figure 2, Table 3). The staining pattern was more fibrillar, in contrast to the linear pattern seen using the HS antibodies.

To study co-localization of specific GAG domains with specific proteoglycans, we analyzed the distribution of seven different core proteins in the kidney (Table 4). Although partial overlap was noticed in a number of cases, no complete overlap was observed between any of the specific GAG domains with any of core proteins studied.

Immunoelectron Microscopy. Four antibodies (HS4C3, EW3D10, HS4E4, and EW4A11) were selected for the ultrastructural localization of specific HS domains, with special emphasis on the glomerulus. The scFv antibody HS4C3 stained the GBM at the site of the podocytes but not of the endothelium (Figure 4A). It also stained the mesangial cells within the glomerulus but not Bowman's capsule (data not shown). In contrast, antibody EW3D10 primarily stained the cell surface of the podocytes, rather than the GBM (Figure 4B). Antibody HS4E4 did not show any staining in the glomerulus (Figure 4C), but it did react with the basal lamina of Bowman's capsule. With antibody EW4A11, no major labeling was observed in the glomerulus.

Involvement of HS Domains on FGF-2 Handling

Staining for endogenous FGF-2 in normal human kidney sections revealed only faint staining of FGF-2. Therefore, kidney cryosections were loaded with FGF-2. FGF-2 primarily bound to the mesangium, to the glomerular tuft, and to a lesser extent to Bowman's capsule (Figure 3A). The ascending thin limbs of Henle's loop and the collecting ducts were also positive for FGF-2 staining. This is in line with observations done by others (25). FGF binding to sections was heparinase III sensitive, indicating that HS is involved in FGF-2 binding.

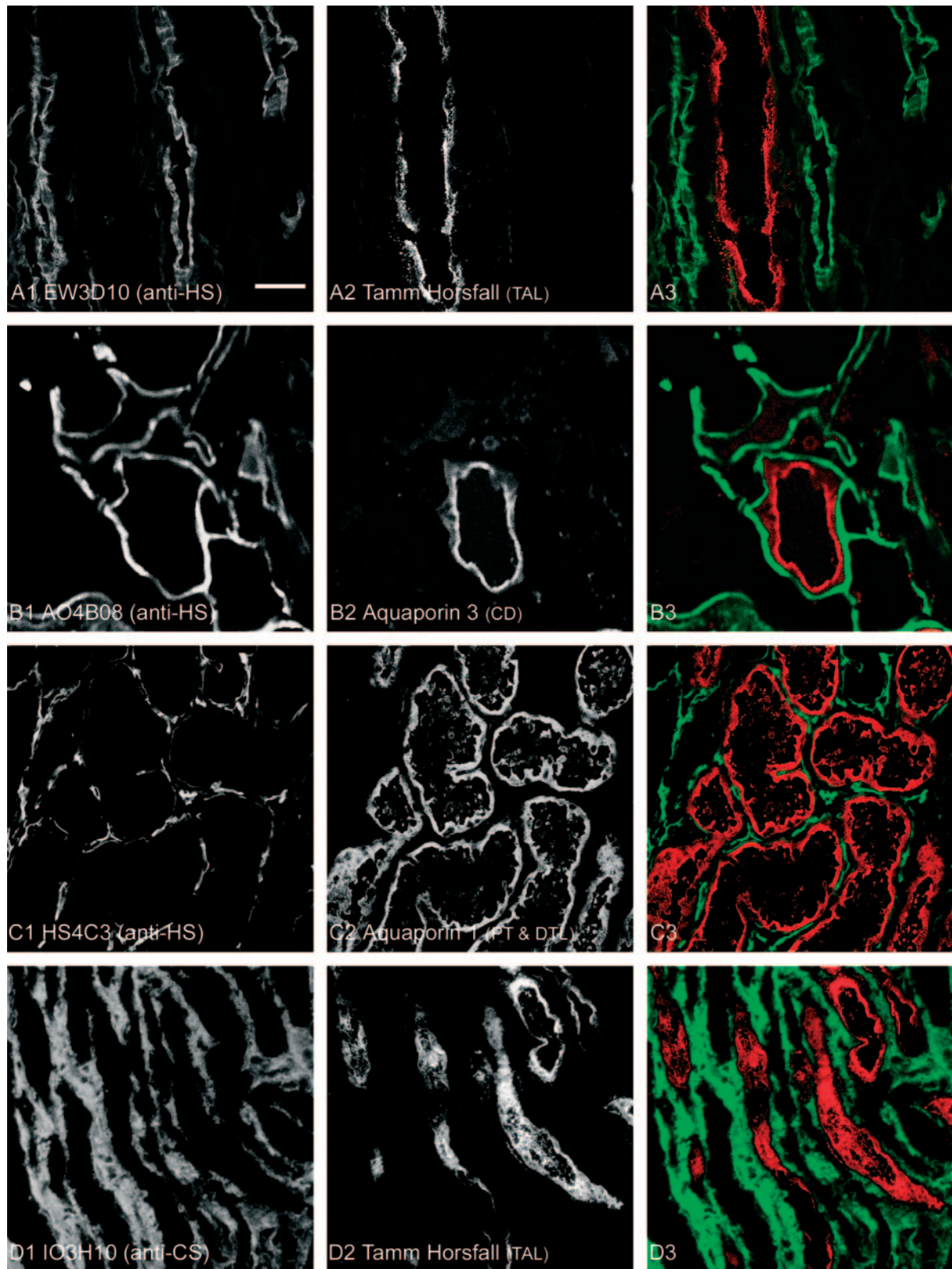


Figure 2. Immunostaining for GAG domains in normal human renal tubules using anti-GAG scFv antibodies. Cryosections were incubated with periplasmic fractions of bacteria that contained the antibodies. (Left) Anti-HS scFv antibody. (Middle) Tubule-specific markers. (Right) Merged image. The antibodies shown are EW3D10 (A1 through A3), AO4B08 (B1 through B3), HS4C3 (C1 through C3), and IO3H10 (D1 through D3). The tubule-specific antibodies used are Tamm-Horsfall (A2 and D2), aquaporin 3 (B2), and aquaporin 1 (C2). TAL, thick ascending limb; CD, collecting duct; PT, proximal tubule; DTL, distal thick limb. Bar = 50 μ m.

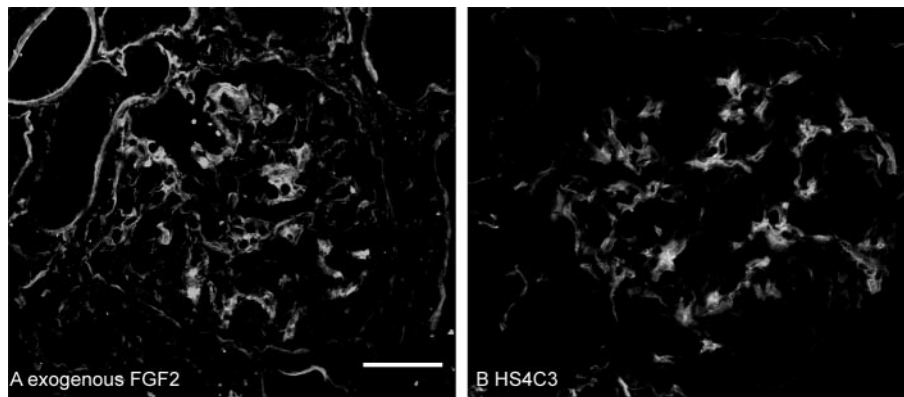


Figure 3. Immunostaining for exogenously applied fibroblast growth factor 2 (FGF-2; A) and HS4C3 (B) in the normal human glomerulus. Bar = 50 μ m.

Table 4. Distribution of proteoglycan core proteins in the normal human kidney^a

Morphologic Structure	Core Protein						
	Versican	Perlecan	Agrin	Endostatin ^b	Syndecan 1	Syndecan 2	Syndecan 3
Glomerular capillary wall	–	–/±	+	–/±	–/±	–	±
Bowman's capsule	+ (matrix)	±	–	+	–	±	±
Mesangium	–	–/±	–	±	–	–	–
PT	–	+	±	+/±	+	–	+
DTL	–	+	±	+/±	+	–	–
Ascending thin limb	–	+	±/+	+/±	±	–	–
TAL	+	++	±	+;++	+	–	±/+
CNT	+	++	±	+;++	±	–	–
CD	+	++	±/+	+;++	±	+	–
Peritubular capillaries	+	+	–	+	–	–	–
Smooth muscle cells	+	–	±	±/+	–	–	+
Blood vessel endothelium	++	++	±	–	–	–	++

^aStaining: ++, strong; +, good; ±, moderate; and –, absent.

^bC-terminal fragment of type XVIII collagen.

To study the involvement of specific HS domains in FGF-2 handling, we selected two scFv antibodies: HS4C3 and RB4Ea12. In a previous study (19), using an ELISA approach, it was shown that the domain defined by scFv antibody HS4C3 was involved in FGF-2 handling, because FGF-2 was able to inhibit the binding of scFv antibody HS4C3 to immobilized HS by 59%. Because the HS4C3 antibody also strongly stained the mesangial area, the site where most FGF-2 staining was found (Figure 3), we selected this antibody for further study using a functional, cell culture approach. We also selected scFv RB4Ea12, because this antibody did not stain the mesangium (Figure 1, Table 3), and FGF-2 did not inhibit binding of this antibody to immobilized HS (data not shown). Both scFv antibodies, however, do stain HMC *in vitro* (Figure 5, A1 and A2). As a control scFv antibody, MPB59 was used (Figure 5C3). This antibody shows, on an amino acid basis, 99% similarity with HS4C3 but is not reactive with HMC or HS (Figure 5C3).

For studying whether FGF-2 is bound to HMC by HS, cells were loaded with FGF-2 with and without previous treatment

with heparinase III. As can be seen from Figure 5B3, FGF-2 binding is heparinase sensitive: No FGF-2 was bound by HMC after enzymatic removal of HS. For studying the effect of FGF-2 on HMC, first the stimulatory effect of FGF-2 was assessed using the WST-1 assay (Figure 6). It was found that 10 ng/ml FGF-2 had a stimulatory effect on HMC proliferation compared with cells that were grown without exogenous FGF-2 (control). The stimulatory effect of FGF-2 was completely counteracted by previous addition of HS4C3 but not by previous addition of RB4Ea12 or MPB59 (Figure 6). Addition of the scFv antibody alone had no effect on HMC proliferation (Figure 6). Previous addition of HS4C3 but not previous addition of RB4Ea12 or MPB59 prevented FGF-2 to bind to HMC (Figure 5, C1 through C3).

Discussion

This study shows that many different GAG domains are located in the adult human kidney. Each domain has a characteristic distribution in the kidney and especially in the nephron. The HS domains are confined to the basement membranes and

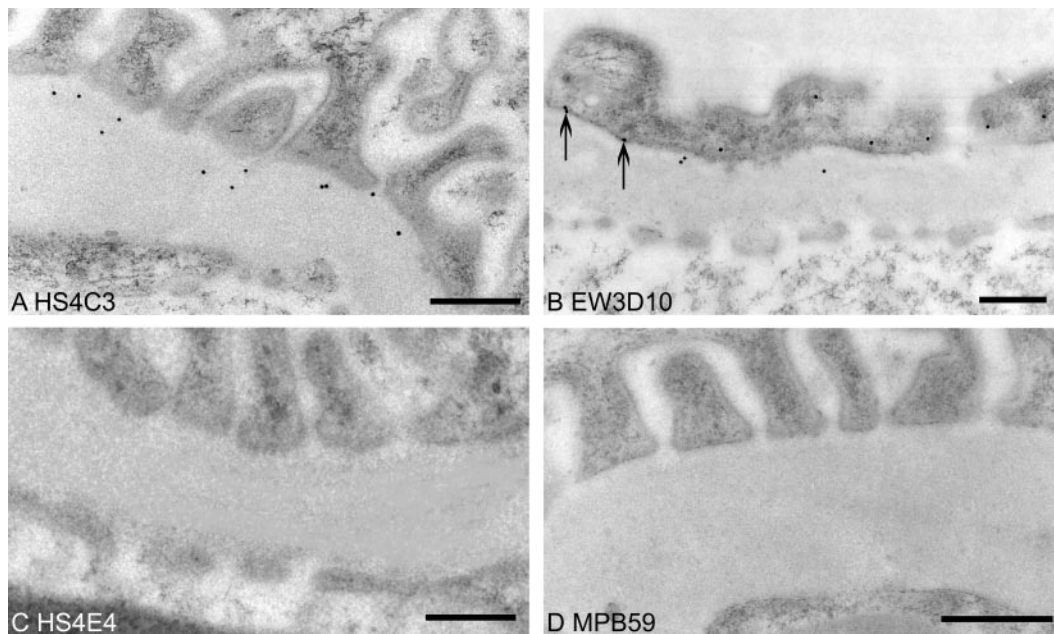


Figure 4. Immunoelectron microscopic staining for HS domains in the normal human glomerulus using anti-HS scFv antibody HS4C3 (A), EW3D10 (B), HS4E4 (C), and the nonrelevant scFv antibody MPB59 (D). The HS domain defined by HS4C3 is present in the glomerular basement membrane (GBM) at the site of the podocytes, whereas the domain defined by EW3D10 is primarily present at the cell surface of the podocytes (arrows in B). Domain HS4E4 is absent in the glomerulus. Bar = 250 nm.

cell surfaces, whereas the CS domain was abundantly expressed in the interstitium but not in the mesangial area. Because seven different scFv antibodies were used, the results indicate that there are at least seven different HS chains in the kidney. Domain heterogeneity within a single chain of HS is also highly likely (1,26). Therefore, in the kidney, an extensive set of different HS domains is present. We studied whether there was a co-localization of a specific core protein and one of the scFv antibodies. Ultrastructural studies indicated some domains to be associated with basement membrane proteoglycans (*e.g.*, domain defined by antibody HS4C3, present in the GBM) and others with cell surface proteoglycans (*e.g.*, domain defined by antibody EW3D10, present at the cell surface of podocytes). However, there was no complete overlap between any of the domains defined by the scFv antibodies and a specific core protein. One explanation for this is that a specific core protein can be substituted with different GAG chains depending on the type of cell (podocyte, endothelium, tubular epithelium, etc.) and its physiologic state (27). In addition, splice variants of core proteins may influence the GAG moiety present in proteoglycans. Immunoprecipitation studies may reveal the core protein(s) to which a specific GAG domain is bound. The location of the domain defined by HS4C3 in the GBM just below the foot processes of the podocytes is of interest regarding the barrier function of the heparan sulfate proteoglycan in the GBM. The antibody recognizes a highly sulfated HS domain and therefore may be involved directly in the charge-dependent permeability characteristics of the glomerulus.

Heparan sulfates bind and modulate a vast amount of proteins (“heparin-binding proteins”) (2,26). These include growth factors such as FGF and vascular endothelial growth factors;

chemokines such as the CXC and CC types; matrix molecules such as collagens and laminins; enzymes such as proteases and lipases; and various enzyme inhibitors (*e.g.*, serpins), receptor proteins (*e.g.*, growth factor receptors), and viral/bacterial proteins. Many of these proteins play an important role in the kidney during health and disease. It is becoming increasingly clear that the protein-binding characteristics of HS cannot be ascribed to a few generic HS molecules but that instead many HS species, each with typical domain structures, exist. A major question is what the cell biologic relevance of the various specific domains is. To address this question, we studied the biologic importance of two domain structures (defined by scFv antibodies HS4C3 and RB4Ea12) with respect to the proliferative effect of FGF-2 on human mesangial cells. We and others have shown that FGF-2 is a potent stimulator of these cells (28). It was found that the HS4C3 but not the RB4Ea12 domain is involved in the binding and handling of FGF-2. ScFv antibody HS4C3 recognizes highly sulfated HS structures that contain O- as well as N-sulfated disaccharides (19). RB4Ea12, however, recognizes low-sulfated oligosaccharides, and 2-O sulfation impedes binding. This is in line with what is known about the structural requirements in the HS domain necessary for FGF binding, in which a 2-O-sulfated IdoA residue is essential. HS has a role in binding both FGF-2 and its receptor (transmembrane tyrosine kinase receptor) (3,29,30). For renal interstitial fibroblasts, the response to FGF-2 is HS mediated (31). Binding of HS to the receptor is dependent on 6-O sulfation; consequently, 2- as well as 6-O sulfation is needed to initiate the signaling events. HS chains, which contain multiple FGF-2 binding sites, may bring together FGF-2 and their receptors in a three-dimensional pattern, such that dimerization, necessary

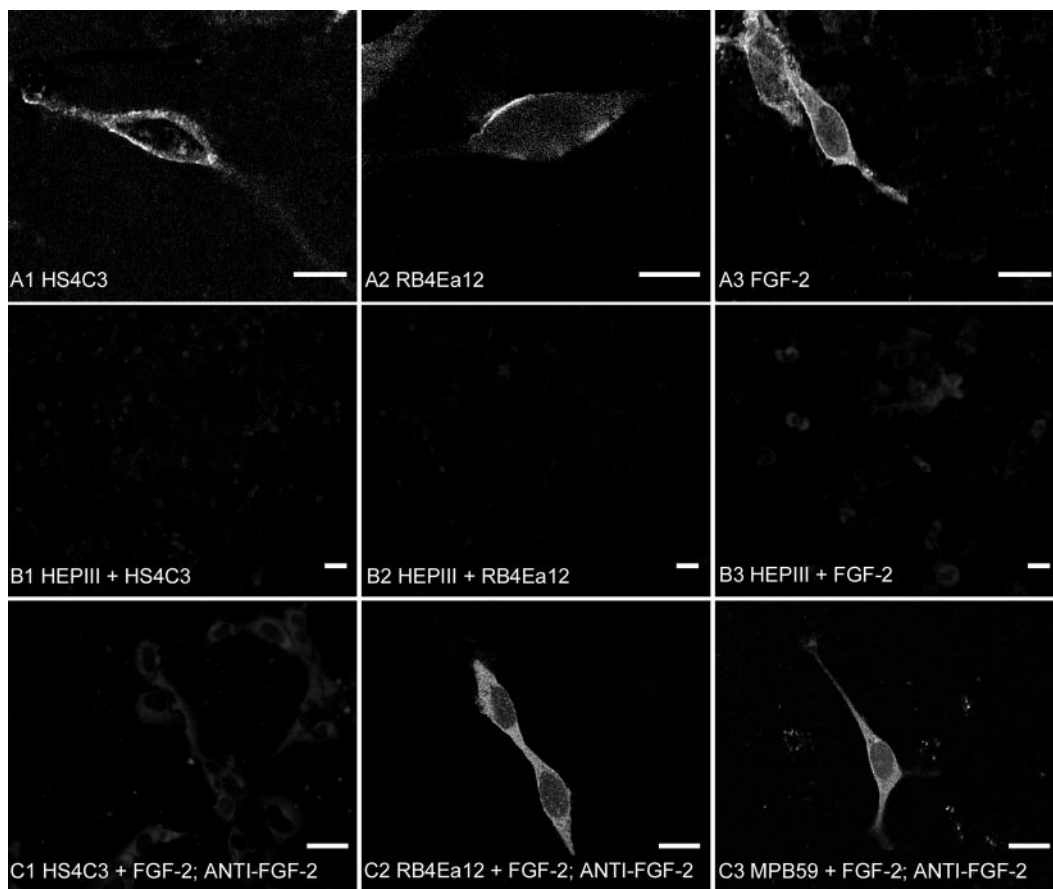


Figure 5. Immunostaining of human mesangial cells (HMC). (A1 through A3) Cells grown in presence of scFv antibodies HS4C3, RB4Ea12, and of FGF-2, respectively. Cells were stained for presence of the scFv antibodies (A1 to A2 and B1 to B2) or for FGF-2 (A3 and B3). (B1 through B3) Cells were pretreated with heparinase III (HepIII) and subsequently treated as A1 through A3. (C1 through C3) Mesangial cells grown in presence of both a scFv antibody and FGF-2 and stained for FGF-2. Note that antibody HS4C3 but not RB4Ea12 inhibits binding of FGF-2 to mesangial cells. MPB59 is a nonrelevant scFv antibody that serves as control (C3). Bar = 20 μ m in A and C and 50 μ m in B.

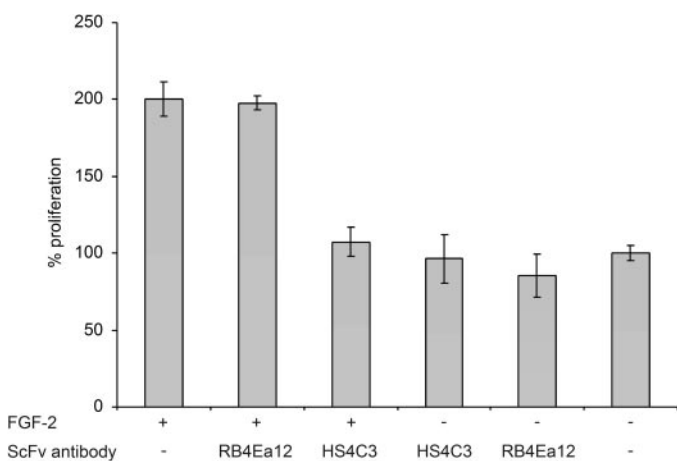


Figure 6. Effect of FGF-2 and purified scFv antibodies, alone or together, on HMC proliferation. Proliferation was measured at 450 nm using the WST-1 test. Incubation conditions of the cells are depicted on the *x* axis, percentage of proliferation on the *y* axis. Proliferation of mesangial cells without FGF-2 and scFv antibody was taken as 100%. Note that only antibody HS4C3 is capable of inhibiting the proliferative effect of FGF-2.

for signal transduction, is established (3,30,32). An effect of the antibodies as such on the signaling events is unlikely because scFv are monovalent and the binding of antibody RB4Ea12 to HMC did not result in any effect. The HS4C3 domain is primarily located in the mesangium, and exogenously applied FGF-2 also concentrates, in an HS-dependent way, in this area. This indicates that *in vivo*, the kidney may use this HS domain to sequester FGF-2 in the mesangium. FGF-2 is involved in a number of renal pathologies, including mesangioproliferative glomerulonephritis (33), tubulointerstitial scarring (34), dysplasia (35), and hemolytic uremic syndrome (36). A specific, FGF-2 binding HS domain, defined by antibody 10E4, was found associated with fibrotic lesions of the peritubular interstitium, further indicating that HS chains with a specific domain structure are involved in FGF-2 handling (37). Knowledge of the chemical structure of HS oligosaccharides involved in FGF-2 handling may lead to the development of glycomimetics for therapeutic use. In this respect, an analogy may be drawn to the development of highly active anticoagulative oligosaccharides (38). The synthesis of these drugs was based on the identification of the chemical structure of a pentasaccharide involved in

the binding of HS/heparin to anti-thrombin III. HS/heparin preparations such as sulodexide and danaparoid have been found to be clinically effective in ameliorating micro- and macroalbuminuria in diabetic nephropathy (39–42). In patients with diabetes, with and without nephropathy, the amount of N-sulfation (as indicated by reactivity with antibody 10E4) was found to be decreased in the urine as well as in the kidney (43). Using the set of scFv antibodies applied in this study, further information can be gathered on structural alterations in HS associated with diabetic nephropathy, eventually leading to a better understanding of the various stages of diabetes and perhaps in better treatment. In addition and because the antibodies used in this study are of a human nature (the phage display library was constructed using human germ line genes), the antibodies may be applied in immunotherapy. Antibodies against FGF-2 have been shown to reduce mesangial cell injury and proliferation in a rat model for mesangial proliferative glomerulonephritis (33).

Some of the scFv antibodies used have also been applied for staining of rat kidney (19–21). In general, a good correlation in staining pattern is seen in human and in rat kidneys, indicating a tight control of HS domain expression. However, some differences are notable. For instance, scFv antibody HS4E4 stained peritubular capillaries in rat but not in human kidney. Differences may be accounted for by variations between species. However, they may also be due to differences in age. The rats used were 3 mo of age (young adults), whereas the human kidneys were from middle-aged individuals (mean, 51 yr). In human aorta, an increase in HS 6-O-sulfation with age has been observed (44) and implicated in the increased binding of PDGF to HS. Age-induced alterations in HS structure may also (functionally?) occur in the kidney and could be demonstrated by the anti-HS scFv antibodies.

In conclusion, a number of structurally different GAG domains with a specific location are present in the normal human kidney and are likely involved in physiologic phenomena. Future research will focus on the chemical identification of the different domains and their role in renal pathobiology.

Acknowledgments

This study was supported by program grant 902-27-292 from The Netherlands Organization for Scientific Research and grant C96.1587 from the Dutch Kidney Foundation.

References

1. Esko JD, Lindahl U: Molecular diversity of heparan sulfate. *J Clin Invest* 108: 169–173, 2001
2. Conrad HE: *Heparin-Binding Proteins*, New York, Academic Press, 1998
3. Tumova S, Woods A, Couchman JR: Heparan sulfate proteoglycans on the cell surface: Versatile coordinators of cellular functions. *Int J Biochem Cell Biol* 32: 269–288, 2000
4. Bernfield M, Gotte M, Park PW, Reizes O, Fitzgerald ML, Lincecum J, Zako M: Functions of cell surface heparan sulfate proteoglycans. *Annu Rev Biochem* 68: 729–777, 1999
5. Forsberg E, Kjellen L: Heparan sulfate: Lessons from knockout mice. *J Clin Invest* 108: 175–180, 2001
6. Li JP, Gong F, Hagner-McWhirter A, Forsberg E, Abrink M, Kisilevsky R, Zhang X, Lindahl U: Targeted disruption of a murine glucuronyl C5-epimerase gene results in heparan sulfate lacking L-iduronic acid and in neonatal lethality. *J Biol Chem* 278: 28363–28366, 2003
7. Filmus J, Selleck SB: Glypicans: Proteoglycans with a surprise. *J Clin Invest* 108: 497–501, 2001
8. van den Born J, van Kraats AA, Bakker MA, Assmann KJ, van den Heuvel LP, Veerkamp JH, Berden JH: Selective proteinuria in diabetic nephropathy in the rat is associated with a relative decrease in glomerular basement membrane heparan sulphate. *Diabetologia* 38: 161–172, 1995
9. Raats CJ, van den Born J, Berden JH: Glomerular heparan sulfate alterations: Mechanisms and relevance for proteinuria. *Kidney Int* 57: 385–400, 2000
10. Stevens FJ, Kisilevsky R: Immunoglobulin light chains, glycosaminoglycans, and amyloid. *Cell Mol Life Sci* 57: 441–449, 2000
11. Conde-Knape K: Heparan sulfate proteoglycans in experimental models of diabetes: A role for perlecan in diabetes complications. *Diabetes Metab Res Rev* 17: 412–421, 2001
12. van den Heuvel LP, Westenend PJ, van den Born J, Assmann KJ, Knoers N, Monnens LA: Aberrant proteoglycan composition of the glomerular basement membrane in a patient with Denys-Drash syndrome. *Nephrol Dial Transplant* 10: 2205–2211, 1995
13. Rops AL, van der Vlag J, Lensen JF, Wijnhoven TJ, van den Heuvel LP, van Kuppevelt TH, Berden JH: Heparan sulfate proteoglycans in glomerular inflammation. *Kidney Int* 65: 768–785, 2004
14. Maccarana M, Sakura Y, Tawada A, Yoshida K, Lindahl U: Domain structure of heparan sulfates from bovine organs. *J Biol Chem* 271: 17804–17810, 1996
15. Saad OM, Leary JA: Compositional analysis and quantification of heparin and heparan sulfate by electrospray ionization ion trap mass spectrometry. *Anal Chem* 75: 2985–2995, 2003
16. Tekotte H, Engel M, Margolis RU, Margolis RK: Disaccharide composition of heparan sulfates: Brain, nervous tissue storage organelles, kidney, and lung. *J Neurochem* 62: 1126–1130, 1994
17. Westling C, Lindahl U: Location of N-unsubstituted glucosamine residues in heparan sulfate. *J Biol Chem* 277: 49247–49255, 2002
18. van den Born J, van den Heuvel LP, Bakker MA, Veerkamp JH, Assmann KJ, Berden JH: Monoclonal antibodies against the protein core and glycosaminoglycan side chain of glomerular basement membrane heparan sulfate proteoglycan: Characterization and immunohistological application in human tissues. *J Histochem Cytochem* 42: 89–102, 1994
19. van Kuppevelt TH, Dennissen MA, van Venrooij WJ, Hoet RM, Veerkamp JH: Generation and application of type-specific anti-heparan sulfate antibodies using phage display technology. Further evidence for heparan sulfate heterogeneity in the kidney. *J Biol Chem* 273: 12960–12966, 1998
20. van de Westerloo EM, Smetsers TF, Dennissen MA, Linhardt RJ, Veerkamp JH, van Muijen GN, van Kuppevelt TH: Human single chain antibodies against heparin: Selection, characterization, and effect on coagulation. *Blood* 99: 2427–2433, 2002
21. Dennissen MA, Jenniskens GJ, Pieffers M, Versteeg EM,

- Petitou M, Veerkamp JH, van Kuppevelt TH: Large, tissue-regulated domain diversity of heparan sulfates demonstrated by phage display antibodies. *J Biol Chem* 277: 10982–10986, 2002
22. Muller M, Marti T, Kriz S: Improved structural preservation by freeze-substitution [Abstract]. *7th European Congress on Electron Microscopy* 2: 720–721, 1980
23. Pieper JS, Hafmans T, van Wachem PB, van Luyn MJ, Brouwer LA, Veerkamp JH, van Kuppevelt TH: Loading of collagen-heparan sulfate matrices with bFGF promotes angiogenesis and tissue generation in rats. *J Biomed Mater Res* 62: 185–194, 2002
24. Banas B, Luckow B, Moller M, Klier C, Nelson PJ, Schadde E, Brigl M, Halevy D, Holthofer H, Reinhart B, Schlondorff D: Chemokine and chemokine receptor expression in a novel human mesangial cell line. *J Am Soc Nephrol* 10: 2314–2322, 1999
25. Floege J, Hudkins KL, Eitner F, Cui Y, Morrison RS, Schelling MA, Alpers CE: Localization of fibroblast growth factor-2 (basic FGF) and FGF receptor-1 in adult human kidney. *Kidney Int* 56: 883–897, 1999
26. Esko JD, Selleck SB: Order out of chaos: Assembly of ligand binding sites in heparan sulfate. *Annu Rev Biochem* 71: 435–471, 2002
27. Kato M, Wang H, Bernfield M, Gallagher JT, Turnbull JE: Cell surface syndecan-1 on distinct cell types differs in fine structure and ligand binding of its heparan sulfate chains. *J Biol Chem* 269: 18881–18890, 1994
28. Gilbert RE, Kelly DJ, McKay T, Chadban S, Hill PA, Cooper ME, Atkins RC, Nikolic-Paterson DJ: PDGF signal transduction inhibition ameliorates experimental mesangial proliferative glomerulonephritis. *Kidney Int* 59: 1324–1332, 2001
29. Ye S, Luo Y, Lu W, Jones RB, Linhardt RJ, Capila I, Toida T, Kan M, Pelletier H, McKeehan WL: Structural basis for interaction of FGF-1, FGF-2, and FGF-7 with different heparan sulfate motifs. *Biochemistry* 40: 14429–14439, 2001
30. Ostrovsky O, Berman B, Gallagher J, Mulloy B, Fernig DG, Delehede M, Ron D: Differential effects of heparin saccharides on the formation of specific fibroblast growth factor (FGF) and FGF receptor complexes. *J Biol Chem* 277: 2444–2453, 2002
31. Clayton A, Thomas J, Thomas GJ, Davies M, Steadman R: Cell surface heparan sulfate proteoglycans control the response of renal interstitial fibroblasts to fibroblast growth factor-2. *Kidney Int* 59: 2084–2094, 2001
32. Maccarana M, Casu B, Lindahl U: Minimal sequence in heparin/heparan sulfate required for binding of basic fibroblast growth factor. *J Biol Chem* 268: 23898–23905, 1993
33. Floege J, Burg M, Hugo C, Gordon KL, Van Goor H, Reidy M, Couser WG, Koch KM, Johnson RJ: Endogenous fibroblast growth factor-2 mediates cytotoxicity in experimental mesangioproliferative glomerulonephritis. *J Am Soc Nephrol* 9: 792–801, 1998
34. Strutz F, Zeisberg M, Hemmerlein B, Sattler B, Hummel K, Becker V, Muller GA: Basic fibroblast growth factor expression is increased in human renal fibrogenesis and may mediate autocrine fibroblast proliferation. *Kidney Int* 57: 1521–1538, 2000
35. Shima H, Tazawa H, Puri P: Increased expression of fibroblast growth factors in segmental renal dysplasia. *Pediatr Surg Int* 16: 306–309, 2000
36. Ray PE, Liu XH, Xu L, Rakusan T: Basic fibroblast growth factor in HIV-associated hemolytic uremic syndrome. *Pediatr Nephrol* 13: 586–593, 1999
37. Morita H, Shinzato T, David G, Mizutani A, Habuchi H, Fujita Y, Ito M, Asai J, Maeda K, Kimata K: Basic fibroblast growth factor-binding domain of heparan sulfate in the human glomerulosclerosis and renal tubulointerstitial fibrosis. *Lab Invest* 71: 528–535, 1994
38. Petitou M, Herault JP, Bernat A, Driguez PA, Duchaussoy P, Lormeau JC, Herbert JM: Synthesis of thrombin-inhibiting heparin mimetics without side effects. *Nature* 398: 417–422, 1999
39. Poplawska A, Szelachowska M, Topolska J, Wysocka-Solowie B, Kinalska I: Effect of glycosaminoglycans on urinary albumin excretion in insulin-dependent diabetic patients with micro- or macroalbuminuria. *Diabetes Res Clin Pract* 38: 109–114, 1997
40. Solini A, Vergnani L, Ricci F, Crepaldi G: Glycosaminoglycans delay the progression of nephropathy in NIDDM. *Diabetes Care* 20: 819–823, 1997
41. Gambaro G, Kinalska I, Oksa A, Pont'uch P, Hertlova M, Olsovsky J, Manitius J, Fedele D, Czekalski S, Perusicova J, Skrha J, Taton J, Grzeszczak W, Crepaldi G: Oral sulodexide reduces albuminuria in microalbuminuric and macroalbuminuric type 1 and type 2 diabetic patients: The Di.N.A.S. randomized trial. *J Am Soc Nephrol* 13: 1615–1625, 2002
42. van der Pijl JW, Lemkes HH, Frolich M, van der Woude FJ, van der Meer FJ, van Es LA: Effect of danaparoid sodium on proteinuria, von Willebrand factor, and hard exudates in patients with diabetes mellitus type 2. *J Am Soc Nephrol* 10: 1331–1336, 1999
43. Yokoyama H, Sato K, Okudaira M, Morita C, Takahashi C, Suzuki D, Sakai H, Iwamoto Y: Serum and urinary concentrations of heparan sulfate in patients with diabetic nephropathy. *Kidney Int* 56: 650–658, 1999
44. Feyzi E, Saldeen T, Larsson E, Lindahl U, Salmivirta M: Age-dependent modulation of heparan sulfate structure and function. *J Biol Chem* 273: 13395–13398, 1998
45. Smetsers TFCM, van de Westerloo EMA, ten Dam GB, Overes IM, Schalkwijk J, van Muijen GNP, van Kuppevelt TH: Human single-chain antibodies reactive with native chondroitin sulfate detect chondroitin sulfate alterations in melanoma and psoriasis. *J Invest Dermatol* 122: 707–716, 2004
46. Nielsen S, Frokiaer J, Marples D, Kwon TH, Agre P, Knepper MA: Aquaporins in the kidney: From molecules to medicine. *Physiol Rev* 82: 205–244, 2002
47. Nielsen S, Kwon TH, Christensen BM, Promeneur D, Frokiaer J, Marples D: Physiology and pathophysiology of renal aquaporins. *J Am Soc Nephrol* 10: 647–663, 1999
48. van den Born J, van den Heuvel LP, Bakker MA, Veerkamp JH, Assmann KJ, Berden JH: Production and characterization of a monoclonal antibody against human glomerular heparan sulfate. *Lab Invest* 65: 287–297, 1991
49. Kriz W, Kaissling B: Structural Organization of the Mammalian Kidney. In: *The Kidney: Physiology and Pathophysiology*, edited by Seldin DW, Giebisch G, New York, Raven Press, 1985, pp 265–306
50. Reilly RF, Ellison DH: Mammalian distal tubule: Physiology, pathophysiology, and molecular anatomy. *Physiol Rev* 80: 277–313, 2000